Measurement of Born cross section of e+e−→Σ+Σ¯− at center-of-mass energies between 3.510 and 4.951 GeV

BESIII Collaboration; Kalantar-Nayestanaki, N.; Kavatsyuk, M.; Messchendorp, J.

Published in:
Journal of High Energy Physics

DOI:
10.1007/JHEP05(2024)022

Document Version
Publisher's PDF, also known as Version of record

Publication date:
2024

Citation for published version (APA):
BESIII Collaboration, Kalantar-Nayestanaki, N., Kavatsyuk, M., & Messchendorp, J. (2024). Measurement of Born cross section of e+e−→Σ+Σ¯− at center-of-mass energies between 3.510 and 4.951 GeV. *Journal of High Energy Physics*, *2024*(5), Article 22. https://doi.org/10.1007/JHEP05(2024)022

Published for SISSA by Springer

Received: *January 19, 2024*
Accepted: *April 7, 2024*
Published: *May 3, 2024*

Measurement of Born cross section of $e^+e^- \to \Sigma^+\bar{\Sigma}^-$ at center-of-mass energies between 3.510 and 4.951 GeV

The BESIII collaboration

E-mail: besiii-publications@ihep.ac.cn

Abstract: Using 24.1 fb^{-1} of e^+e^- collision data collected with the BESIII detector at the BEPCII collider, the Born cross sections and effective form factors of the $e^+e^- \to \Sigma^+\bar{\Sigma}^-$ reaction are measured. The measurements are performed at center-of-mass energies ranging from 3.510 to 4.951 GeV. No significant evidence for the decay of the charmonium(-like) states, $\psi(3770)$, $\psi(4040)$, $\psi(4160)$, $Y(4230)$, $Y(4360)$, $\psi(4415)$, and $Y(4660)$, into a $\Sigma^+\bar{\Sigma}^-$ final state is observed. Consequently, upper limits for the products of the branching fractions and the electronic partial widths at the 90% confidence level are reported for these decays.

Keywords: e^+-e^- Experiments, QCD, Branching fraction, Electroweak Interaction

ArXiv ePrint: 2401.09468

https://doi.org/10.1007/JHEP05(2024)022

Contents

1 Introduction

Below open-charm threshold, the mass spectrum of conventional charmonium states aligns with the potential quark model [1]. According to this model, there exist five vector charmonium states between the 1D state ($\psi(3770)$) and 4.7 GeV/c^2, specifically identified as the 3S, 2D, 4S, 3D, and 5S states [2]. However, within this energy range, an overabundance of vector states have been detected. Among them, three (conventional) states, namely $\psi(4040)$, $\psi(4160)$ and $\psi(4415)$ [3], the 3S, 2D, and 4S states, respectively, are primarily characterized as open-charm states. In addition, four new (non-conventional) states, i.e. $Y(4230)$, $Y(4360)$, $Y(4634)$, and $Y(4660)$, are predominantly observed in hidden-charm final states. These states are generated via initial state radiation (ISR) processes at BaBar and Belle [4–12], or by direct production processes at CLEO [13] and BESIII [14, 15]. The overpopulation of structures in this mass region and the mismatch of the properties between the potential model predictions and experimental measurements make them good candidates for exotic states. Many hypotheses have been proposed to explain their nature [2, 16–23], including the possibility of being hybrid states, multiple-quark states, or even molecular structures. In particular, charmless decays of these non-conventional states are proposed by the hybrid model [16]. On the other hand, if these states are considered as pure charmonium [19], their baryonic decays, which have not yet been observed, would provide important information to validate the scenario as suggested in ref. [20].

The complex situation reflects our limited understanding of the strong interaction, particularly in its non-perturbative aspects. In order to address this challenging problem, it is imperative to make additional experimental measurements, and the study of $\psi/Y \to B\bar{B}$ decays holds great promise. These decays exhibit a straightforward topology in terms of the final states, and the underlying interaction mechanism is assumed to be dominated by three-gluon or one-photon processes. Additionally, investigations into the electromagnetic form factors or effective form factors of $B\bar{B}$ pairs have the potential to provide insight into the internal composition of charmonium(-like) states. Although many experimental studies [8, 24–31] of $B\bar{B}$ pair production in this energy region have been performed by the BESIII and Belle experiments, except for two evidences of $\psi(3770) \to \Lambda\bar{\Lambda}$ and $\Xi^-\bar{\Xi}^+$, no significant indication for $B\bar{B}$ decay of other vector charmonium(-like) states has been found. Thus, more precise measurements of exclusive cross sections for $B\bar{B}$ final states above the open-charm threshold are crucial.

This paper reports the measurements of the Born cross section and the effective form factor for the process of $e^+e^- \to \Sigma^+\bar{\Sigma}^-$ using the data corresponding to a total integrated luminosity of 24.1 fb^{-1} collected at center-of-mass (CM) energies ($\sqrt{s}$) between 3.510 and 4.951 GeV with the BESIII detector [32] at the BEPCII collider [33]. In addition, potential resonances are searched for by fitting the dressed cross section of the $e^+e^- \to \Sigma^+\bar{\Sigma}^-$ reaction.

2 BESIII detector and Monte Carlo simulation

The BESIII detector [32] records symmetric e^+e^- collisions provided by the BEPCII storage ring [33] in the range of $\sqrt{s}$ from 2.0 to 4.95 GeV, with a peak luminosity of $1 \times 10^{33}\,\mathrm{cm}^{-2}\,\mathrm{s}^{-1}$ achieved at $\sqrt{s} = 3.77$ GeV. BESIII has collected large data samples in this energy region [34–36]. The cylindrical core of the BESIII detector covers 93% of the full solid angle and consists of a helium-based multilayer drift chamber (MDC), a plastic scintillator time-of-flight system (TOF), and a CsI(Tl) electromagnetic calorimeter (EMC), which are all enclosed in a superconducting solenoidal magnet providing a 1.0 T magnetic field. The solenoid is supported by an octagonal flux-return yoke with resistive plate counter muon identification modules interleaved with steel. The charged-particle momentum resolution at 1 GeV/c is 0.5%, and the dE/dx resolution is 6% for electrons from Bhabha scattering. The EMC measures photon energies with a resolution of 2.5% (5%) at 1 GeV in the barrel (end cap) region. The time resolution in the TOF barrel region is 68 ps, while that in the end cap region was 110 ps. The end cap TOF system was upgraded in 2015 using multigap resistive plate chamber technology, providing a time resolution of 60 ps [37–39] and benefiting 82% of the data used in this analysis.

To evaluate detection efficiencies and estimate backgrounds, simulated data samples are produced using GEANT4-based Monte Carlo (MC) software [40], which incorporates the geometric description of the BESIII detector [41] as well as the detector response. The simulation of the $e^+e^- \to \Sigma^+\bar{\Sigma}^-$ production process models the beam energy spread in the e^+e^- annihilation process, employing KKMC [42]. For each of the 41 CM energy points ranging from 3.510 to 4.951 GeV, a sample of 100,000 events is simulated with a uniform phase space (PHSP) distribution. The $\Sigma^+\bar{\Sigma}^-$ baryon pair and their subsequent decays are simulated using EVTGEN [43, 44] with a PHSP model.

3 Event selection

Due to the large background in the selection of $e^+e^- \to \Sigma^+\bar{\Sigma}^-$ events, both the Σ^+ and $\bar{\Sigma}^-$ are required to be reconstructed via the decay modes $\Sigma^+ \to p\pi^0$ and $\bar{\Sigma}^- \to \bar{p}\pi^0$ with the subsequent decay $\pi^0 \to \gamma\gamma$.

Tracks of charged particles detected in the MDC are required to lie within the angular coverage of the MDC $|\cos\theta| < 0.93$, where θ is the angle between the charged track and the z axis, which is the symmetry axis of the MDC. At least one positively charged and one negatively charged track are required to be reconstructed in the MDC with good Kalman fits. Because the proton and anti-proton can be separated according to their momenta in a $\Sigma^+\bar{\Sigma}^-$ decay, a charged particle with momentum greater than $0.5\,\mathrm{GeV}/c$ is identified as a proton or anti-proton.

For π^0 reconstruction, the energies of photons are required to be greater than 25 MeV in the EMC barrel region ($|\cos\theta| < 0.8$) and greater than 50 MeV in the EMC end cap ($0.86 < |\cos\theta| < 0.92$). To suppress electronic noise and energy deposits unrelated to the events, the EMC shower time measured with respect to the collision signal, is required to satisfy $0 < t < 700$ ns. After these selections, at least four photons are required.

The best candidate of all combinations of $p\bar{p}\gamma\gamma\gamma\gamma$ within an event is determined by a six-constraint (6C) kinematic fit, which imposes energy and momentum conservation and constrains the masses of photon pairs to the known mass of π^0 [45]. The $p\bar{p}\pi^0\pi^0$ combination with the smallest fit χ^2 is chosen. For different $p(\bar{p})$ and π^0 combinations, the Σ^+ and $\bar{\Sigma}^-$ pair with the minimum of $\sqrt{(M_{p\pi^0} - m_{\Sigma^+})^2 + (M_{\bar{p}\pi^0} - m_{\bar{\Sigma}^-})^2}$, is selected. Here, $M_{p\pi^0(\bar{p}\pi^0)}$ is the invariant mass of the $p\pi^0(\bar{p}\pi^0)$ combination, and $m_{\Sigma^+(\bar{\Sigma}^-)}$ is the known mass of $\Sigma^+(\bar{\Sigma}^-)$ from the Particle Data Group (PDG) [45]. Figure 1 shows the distributions of $M_{p\pi^0}$ versus $M_{\bar{p}\pi^0}$ for each energy point and the sum of all energy points. $M_{p\pi^0(\bar{p}\pi^0)}$ is required to be within the range of $[m_{\Sigma^+} - 4\sigma, m_{\Sigma^+} + 3\sigma]$, which is labeled by S in figure 1. The resolution σ and the signal region are determined by a fit with the Crystal-Ball function [46]. Due to the longer tail of the photon energy deposition at the low energy side in the EMC, the signal region is asymmetric.

4 Born cross section measurement

4.1 Determination of signal yields

After applying the event selection criteria on data, the remaining background mainly comes from non-$\Sigma^+\bar{\Sigma}^-$ events, such as $e^+e^- \to \pi^0\pi^0 J/\psi \to \pi^0\pi^0 p\bar{p}$. To estimate the background yield in the signal region, four sideband regions B_i (where $i = 1, 2, 3, 4$) are utilized. These sideband regions, shown in figure 1, have the same area as the signal region, and the exact ranges are defined by

- B_1: $M_{p\pi^0} \in [1.119,\ 1.154]$ GeV/c^2 & $M_{\bar{p}\pi^0} \in [1.219,\ 1.254]$ GeV/c^2,
- B_2: $M_{p\pi^0} \in [1.219,\ 1.254]$ GeV/c^2 & $M_{\bar{p}\pi^0} \in [1.219,\ 1.254]$ GeV/c^2,

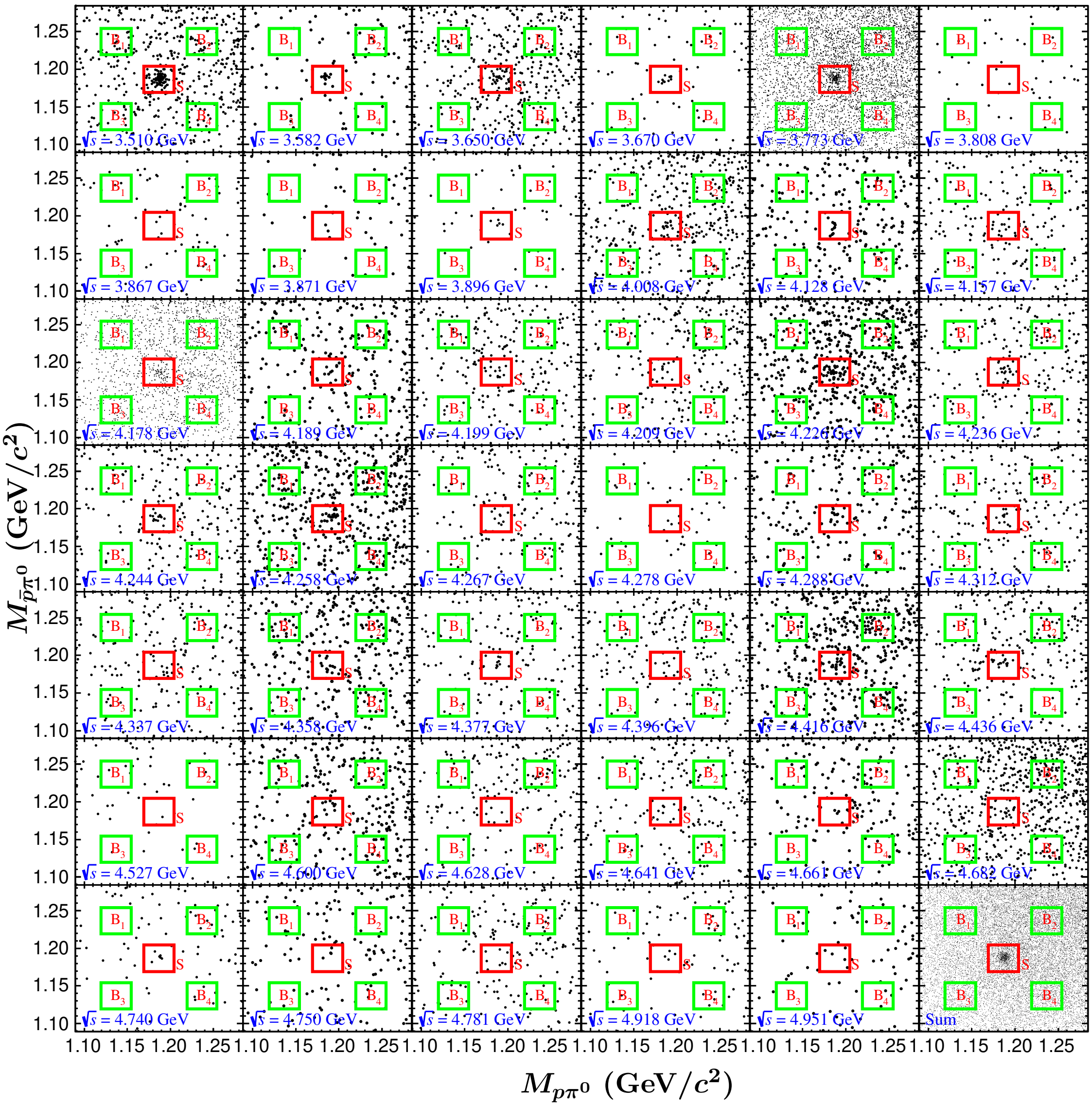

Figure 1. Distributions of $M_{p\pi^0}$ versus $M_{\bar{p}\pi^0}$ for data at each energy point between 3.510 and 4.951 GeV and the sum of all energy points (bottom right) from data. The red boxes represent the signal regions and the green boxes represent the selected sideband regions.

- B_3: $M_{p\pi^0} \in [1.119,\ 1.154]$ GeV/c^2 & $M_{\bar{p}\pi^0} \in [1.119,\ 1.154]$ GeV/c^2,
- B_4: $M_{p\pi^0} \in [1.219,\ 1.254]$ GeV/c^2 & $M_{\bar{p}\pi^0} \in [1.119,\ 1.154]$ GeV/c^2.

The signal yield $N_{\rm obs}$ for the $e^+e^- \to \Sigma^+\bar{\Sigma}^-$ reaction at each energy point is determined by subtracting the number of events in the sideband regions from the signal region, i.e., $N_{\rm obs} = N_S - N_{\rm bkg}$, where N_S is the number of events from the signal region and $N_{\rm bkg} = \frac{1}{4}\sum_{i=1}^{4} N_{B_i}$. Statistical uncertainties are calculated based on the TRolke method [49], and the statistical significance is evaluated based on the observed p-value [48]. The results are listed in table 1. For the energy points with statistical significance less than 3σ, the upper limit at the 90% confidence level (C.L.) is also estimated based on the TRolke method, which takes into account systematic uncertainties.

4.2 Determination of Born cross section and effective form factor

The Born cross section for the $e^+e^- \to \Sigma^+\bar{\Sigma}^-$ process at a given CM energy is calculated by

$$\sigma^B = \frac{N_{\rm obs}}{\mathcal{L} \cdot (1+\delta) \cdot \frac{1}{|1-\prod|^2} \cdot \epsilon \cdot \mathcal{B}^2_{\Sigma^+\to p\pi^0} \cdot \mathcal{B}^2_{\pi^0\to\gamma\gamma}}, \tag{4.1}$$

where $N_{\rm obs}$ is the number of observed signal events, $\mathcal{L}$ is the integrated luminosity, $(1+\delta)$ is the ISR correction factor, $\frac{1}{|1-\Pi|^2}$ is the vacuum polarization (VP) correction factor, ϵ is the detection efficiency, and $\mathcal{B}_{\Sigma^+\to p\pi^0}$ and $\mathcal{B}_{\pi^0\to\gamma\gamma}$ are the PDG branching fractions [45]. The ISR correction factor is obtained using the QED calculation as described in ref. [50], and the VP correction factor is calculated according to ref. [51]. The efficiency and ISR correction factor are obtained through an iterative process. Initially, the cross section is measured without any correction factors. Using this initial line shape, signal MC samples are regenerated, and their efficiencies and ISR correction factors are recalculated. Subsequently, the Born cross section of $e^+e^- \to \Sigma^+\bar{\Sigma}^-$ is updated and used as input for the next iteration. To expedite the iteration procedure, an iterative weighting method, as proposed in ref. [52], is employed. The procedure is iteratively performed until the difference of $\epsilon \cdot (1+\delta)$ with the last iteration falls below 0.5%. The results of the measured Born cross sections and the Σ^+ effective form factors $G_{\rm eff}(s)$ for different energy points are listed in table 2. $G_{\rm eff}(s)$ is defined as [26]

$$|G_{\rm eff}(s)| = \sqrt{\frac{3s\tau\sigma^B}{2\pi\alpha^2 C\beta(2\tau+1)}}, \tag{4.2}$$

where s is the square of the CM energy, $\alpha = \frac{1}{137}$ is the fine structure constant, the variable $\beta = \sqrt{1-\frac{1}{\tau}}$ is the velocity of Σ^+ in the laboratory department, $\tau = \frac{s}{4m^2_{\Sigma^+}}$, and the Coulomb factor C [53, 54] parameterizes the electromagnetic interaction between the outgoing baryon and anti-baryon. For neutral baryons, the Coulomb factor is unity, while for point-like charged fermions, $C = \frac{\pi\alpha}{\beta} \cdot \frac{\sqrt{1-\beta^2}}{1-e^{-\frac{\pi\alpha}{\beta}}}$ [55–58]. Figure 2 displays the energy dependence of the Born cross section and Σ^+ effective form factor $G_{\rm eff}(s)$ measurements, as well as a comparison of the Born cross sections and the effective form factors with the CLEO-c results [59] at $\sqrt{s} = 3.770$ and 4.160 GeV.

5 Systematic uncertainty

The systematic uncertainties on the Born cross section measurements mainly originate from the integrated luminosity, $\Sigma^+(\bar{\Sigma}^-)$ reconstruction, background, angular distribution, branching fractions, and input line shape.

5.1 Luminosity

The luminosity at all energy points is measured using Bhabha events with the uncertainties of 1.0% [60] below 4.0 GeV, 0.7% [61] from 4.0 to 4.6 GeV and 0.5% [62] above 4.6 GeV, which are taken as the systematic uncertainties due to the luminosity measurement.

$\sqrt{s}$ (GeV)	N_S	$N_{\rm bkg}$	$N_{\rm obs}$ ($< N^{\rm UL}$)	$\mathcal{S}$ (σ)
3.510	$89.0^{+10.5}_{-9.4}$	$18.8^{+5.1}_{-4.6}$	$70.3^{+10.5}_{-8.4}$	7.9
3.582	$12.0^{+4.6}_{-3.4}$	$4.0^{+3.2}_{-1.9}$	$8.0^{+3.8}_{-3.1}$	3.3
3.650	$44.0^{+7.7}_{-6.6}$	$10.0^{+4.3}_{-3.1}$	$34.0^{+7.0}_{-6.3}$	7.9
3.670	$13.0^{+4.7}_{-3.6}$	$2.8^{+2.5}_{-1.8}$	$10.3^{+4.7}_{-2.5}$	4.5
3.773	$324.0^{+19.0}_{-18.0}$	$139.3^{+12.5}_{-12.1}$	$184.8^{+18.6}_{-17.4}$	7.9
3.808	$2.0^{+2.6}_{-1.3}$	$1.3^{+2.0}_{-1.1}$	$0.8^{+2.0}_{-0.8}$ (< 4.5)	0.9
3.867	$4.0^{+3.2}_{-1.9}$	$3.3^{+2.6}_{-1.9}$	$0.8^{+2.6}_{-0.8}$ (< 5.8)	0.8
3.871	$4.0^{+3.2}_{-1.9}$	$1.0^{+2.3}_{-0.8}$	$3.0^{+2.3}_{-1.7}$ (< 7.5)	2.3
3.896	$6.0^{+3.6}_{-2.4}$	$1.5^{+2.5}_{-1.1}$	$4.5^{+3.3}_{-1.6}$ (< 10.2)	2.8
4.008	$29.0^{+6.4}_{-5.4}$	$11.3^{+4.1}_{-3.6}$	$17.8^{+6.0}_{-4.8}$	4.5
4.128	$13.0^{+4.7}_{-3.6}$	$6.5^{+3.7}_{-2.5}$	$6.5^{+4.4}_{-2.8}$ (< 14.8)	2.4
4.157	$16.0^{+5.1}_{-4.0}$	$4.3^{+2.9}_{-2.2}$	$11.8^{+4.6}_{-3.4}$	4.4
4.178	$99.0^{+11.0}_{-9.9}$	$54.5^{+8.4}_{-7.4}$	$44.5^{+10.8}_{-9.1}$	5.5
4.189	$12.0^{+4.6}_{-3.4}$	$9.0^{+4.1}_{-2.9}$	$3.0^{+3.8}_{-3.0}$ (< 10.9)	1.3
4.199	$15.0^{+5.0}_{-3.8}$	$7.8^{+3.6}_{-3.0}$	$7.3^{+5.0}_{-2.8}$ (< 16.3)	2.5
4.209	$14.0^{+4.8}_{-3.7}$	$7.8^{+3.6}_{-3.0}$	$6.3^{+4.8}_{-2.7}$ (< 15.1)	2.2
4.226	$45.0^{+7.8}_{-6.7}$	$16.0^{+5.1}_{-4.0}$	$29.0^{+7.0}_{-6.4}$	6.0
4.236	$21.0^{+5.7}_{-4.5}$	$9.0^{+4.1}_{-2.9}$	$12.0^{+4.9}_{-4.3}$	3.5
4.244	$16.0^{+5.1}_{-4.0}$	$6.8^{+3.4}_{-2.8}$	$9.3^{+5.1}_{-2.9}$	3.1
4.258	$28.0^{+6.4}_{-5.3}$	$19.8^{+5.2}_{-4.7}$	$8.3^{+6.4}_{-4.2}$ (< 20.7)	2.0
4.267	$13.0^{+4.7}_{-3.6}$	$7.0^{+3.8}_{-2.6}$	$6.0^{+3.9}_{-3.3}$ (< 13.9)	2.2
4.278	$5.0^{+3.4}_{-2.2}$	$3.0^{+2.9}_{-1.6}$	$2.0^{+2.6}_{-2.0}$ (< 7.2)	1.3
4.288	$17.0^{+5.2}_{-4.1}$	$8.3^{+3.6}_{-3.1}$	$8.8^{+4.7}_{-3.5}$ (< 17.9)	2.8
4.312	$15.0^{+5.0}_{-3.8}$	$8.0^{+3.9}_{-2.8}$	$7.0^{+4.2}_{-3.5}$ (< 15.5)	2.4
4.337	$13.0^{+4.7}_{-3.6}$	$5.8^{+3.2}_{-2.6}$	$7.3^{+4.7}_{-2.5}$ (< 15.7)	2.7
4.358	$16.0^{+5.1}_{-4.0}$	$13.8^{+4.5}_{-3.9}$	$2.3^{+5.1}_{-2.2}$ (< 12.2)	1.0
4.377	$14.0^{+4.8}_{-3.7}$	$6.3^{+3.3}_{-2.7}$	$7.8^{+4.3}_{-3.2}$ (< 16.0)	2.8
4.396	$11.0^{+4.4}_{-3.3}$	$7.3^{+3.5}_{-2.9}$	$3.8^{+3.9}_{-3.8}$ (< 11.5)	1.6
4.416	$26.0^{+6.2}_{-5.1}$	$19.0^{+5.4}_{-4.3}$	$7.0^{+5.4}_{-4.8}$ (< 18.4)	1.8
4.436	$17.0^{+5.2}_{-4.1}$	$8.8^{+3.7}_{-3.2}$	$8.3^{+5.2}_{-3.0}$ (< 17.9)	2.6
4.527	$3.0^{+2.9}_{-1.6}$	$2.5^{+2.8}_{-1.5}$	$0.5^{+2.6}_{-0.5}$ (< 5.2)	0.7
4.600	$11.0^{+4.4}_{-3.3}$	$10.5^{+4.3}_{-3.2}$	$0.5^{+4.2}_{-0.5}$ (< 8.8)	0.7
4.628	$7.0^{+3.8}_{-2.6}$	$6.5^{+3.7}_{-2.5}$	$0.5^{+3.5}_{-0.5}$ (< 7.3)	0.7
4.641	$12.0^{+4.6}_{-3.4}$	$6.3^{+3.3}_{-2.7}$	$5.8^{+4.1}_{-2.9}$ (< 13.6)	2.2
4.661	$8.0^{+3.9}_{-2.8}$	$6.0^{+3.6}_{-2.4}$	$2.0^{+3.2}_{-2.0}$ (< 8.6)	1.1
4.682	$26.0^{+6.2}_{-5.1}$	$21.8^{+5.4}_{-4.9}$	$4.3^{+6.2}_{-4.2}$ (< 16.6)	1.3
4.740	$7.0^{+3.8}_{-2.6}$	$3.3^{+2.6}_{-1.9}$	$3.8^{+3.2}_{-2.1}$ (< 9.9)	2.0
4.750	$4.0^{+3.2}_{-1.9}$	$3.5^{+3.0}_{-1.8}$	$0.5^{+2.8}_{-0.5}$ (< 5.8)	0.7
4.781	$10.0^{+4.3}_{-3.1}$	$6.5^{+3.7}_{-2.5}$	$3.5^{+4.0}_{-2.3}$ (< 11.1)	1.5
4.918	$5.0^{+3.4}_{-2.2}$	$4.5^{+3.3}_{-2.0}$	$0.5^{+3.1}_{-0.5}$ (< 6.4)	0.7
4.951	$5.0^{+3.4}_{-2.2}$	$2.0^{+2.6}_{-1.3}$	$3.0^{+2.6}_{-1.9}$ (< 8.0)	1.9

Table 1. Number of events: N_S is from the signal region, $N_{\rm bkg}$ is the number of background events, $N_{\rm obs}$ is the number of events by subtracting the backgrounds, $S(\sigma)$ is the statistical significance, and $N^{\rm UL}$ is the upper limit for an energy point with statistical significance less than 3σ.

$\sqrt{s}$ (GeV)	$\mathcal{L}$ (pb^{-1})	$\frac{1}{\lvert 1-\prod \rvert^2}$	$\epsilon \cdot (1+\delta)$	$N_{\rm obs}$ ($< N^{\rm UL}$)	σ^B (fb)	$\lvert G_{\rm eff}(s) \rvert$ $\times 10^{-3}$	$\mathcal{S}$ (σ)
3.510	405.4	1.04	0.25	$70.3^{+10.5}_{-8.4}$	$2517.9^{+376.3}_{-301.1} \pm 103.2$	$23.9^{+1.8}_{-1.4} \pm 0.5$	7.9
3.582	85.7	1.04	0.25	$8.0^{+3.8}_{-3.1}$	$1366.3^{+649.0}_{-529.4} \pm 56.0$	$18.1^{+4.3}_{-3.5} \pm 0.4$	3.3
3.650	410.0	1.02	0.25	$34.0^{+7.0}_{-6.3}$	$1236.5^{+254.6}_{-229.1} \pm 50.7$	$17.6^{+1.8}_{-1.6} \pm 0.4$	7.9
3.670	84.7	0.99	0.25	$10.3^{+4.7}_{-2.5}$	$1866.2^{+855.7}_{-455.2} \pm 76.5$	$21.8^{+5.0}_{-2.7} \pm 0.4$	4.5
3.773	2931.8	1.06	0.26	$184.8^{+18.6}_{-17.4}$	$891.4^{+89.7}_{-84.0} \pm 36.5$	$15.6^{+0.8}_{-0.7} \pm 0.3$	7.9
3.808	50.5	1.06	0.26	$0.8^{+2.0}_{-0.8}$ (< 4.5)	$211.4^{+563.8}_{-225.5} \pm 8.7$ (< 1268.5)	$7.7^{+10.3}_{-4.1} \pm 0.2$ (< 18.9)	0.9
3.867	108.9	1.05	0.25	$0.8^{+2.6}_{-0.8}$ (< 5.8)	$99.4^{+344.7}_{-106.1} \pm 4.1$ (< 768.9)	$5.4^{+9.4}_{-2.9} \pm 0.1$ (< 15.0)	0.8
3.871	110.3	1.05	0.26	$3.0^{+2.3}_{-1.7}$ (< 7.5)	$390.4^{+299.3}_{-221.2} \pm 16.0$ (< 976.1)	$10.7^{+4.1}_{-3.0} \pm 0.2$ (< 17.0)	2.3
3.896	52.6	1.05	0.26	$4.5^{+3.3}_{-1.6}$ (< 10.2)	$1222.3^{+896.4}_{-434.6} \pm 50.1$ (< 2770.5)	$19.1^{+7.0}_{-3.4} \pm 0.4$ (< 28.8)	2.8
4.008	482.0	1.04	0.26	$17.8^{+6.0}_{-4.8}$	$527.6^{+178.4}_{-142.7} \pm 21.6$	$13.1^{+2.2}_{-1.8} \pm 0.3$	4.5
4.128	401.5	1.05	0.26	$6.5^{+4.4}_{-2.8}$ (< 14.8)	$231.3^{+156.6}_{-99.6} \pm 9.5$ (< 526.6)	$9.0^{+3.1}_{-1.9} \pm 0.2$ (< 13.6)	2.4
4.157	408.7	1.05	0.26	$11.8^{+4.6}_{-3.4}$	$411.5^{+161.1}_{-119.1} \pm 16.9$	$12.1^{+2.4}_{-1.8} \pm 0.2$	4.4
4.178	3189.0	1.05	0.25	$44.5^{+10.8}_{-9.1}$	$202.7^{+49.2}_{-41.5} \pm 8.3$	$8.6^{+1.0}_{-0.9} \pm 0.2$	5.5
4.189	526.7	1.06	0.25	$3.0^{+3.8}_{-3.0}$ (< 10.9)	$82.3^{+104.2}_{-82.3} \pm 3.4$ (< 298.9)	$5.5^{+3.5}_{-2.7} \pm 0.1$ (< 10.5)	1.3
4.199	526.0	1.06	0.25	$7.3^{+5.0}_{-2.8}$ (< 16.3)	$198.0^{+136.6}_{-76.5} \pm 8.1$ (< 445.2)	$8.5^{+2.9}_{-1.6} \pm 0.2$ (< 12.8)	2.5
4.209	517.1	1.06	0.25	$6.3^{+4.8}_{-2.7}$ (< 15.1)	$173.1^{+133.0}_{-74.8} \pm 7.1$ (< 418.3)	$8.0^{+3.1}_{-1.7} \pm 0.2$ (< 12.5)	2.2
4.226	1100.9	1.06	0.25	$29.0^{+7.0}_{-6.4}$	$377.3^{+91.1}_{-83.3} \pm 15.5$	$11.9^{+1.4}_{-1.3} \pm 0.2$	6.0
4.236	530.3	1.06	0.25	$12.0^{+4.9}_{-4.3}$	$327.4^{+133.7}_{-117.3} \pm 13.4$	$11.1^{+2.3}_{-2.0} \pm 0.2$	3.5
4.244	538.1	1.06	0.25	$9.3^{+5.1}_{-2.9}$	$248.3^{+136.9}_{-77.9} \pm 10.2$	$9.7^{+2.7}_{-1.5} \pm 0.2$	3.1
4.258	828.4	1.05	0.25	$8.3^{+6.4}_{-4.2}$ (< 20.7)	$143.0^{+111.0}_{-72.8} \pm 5.9$ (< 358.9)	$7.4^{+2.9}_{-1.9} \pm 0.2$ (< 11.7)	2.0
4.267	531.1	1.05	0.25	$6.0^{+3.9}_{-3.3}$ (< 13.9)	$162.7^{+105.8}_{-89.5} \pm 6.7$ (< 377.0)	$7.9^{+2.6}_{-2.2} \pm 0.2$ (< 12.1)	2.2
4.278	175.7	1.05	0.25	$2.0^{+2.6}_{-2.0}$ (< 7.2)	$164.9^{+214.3}_{-164.9} \pm 6.8$ (< 593.6)	$8.0^{+5.2}_{-4.0} \pm 0.2$ (< 15.2)	1.3
4.288	502.4	1.05	0.26	$8.8^{+4.7}_{-3.5}$ (< 17.9)	$249.3^{+133.9}_{-99.7} \pm 10.2$ (< 509.9)	$9.9^{+2.7}_{-2.0} \pm 0.2$ (< 14.1)	2.8
4.312	501.2	1.05	0.25	$7.0^{+4.2}_{-3.5}$ (< 15.5)	$201.4^{+120.8}_{-100.7} \pm 8.3$ (< 445.9)	$8.9^{+2.7}_{-2.2} \pm 0.2$ (< 13.3)	2.4
4.337	505.0	1.05	0.25	$7.3^{+4.7}_{-2.5}$ (< 15.7)	$208.6^{+135.2}_{-71.9} \pm 8.6$ (< 451.7)	$9.2^{+3.0}_{-1.6} \pm 0.2$ (< 13.5)	2.7
4.358	544.0	1.05	0.24	$2.3^{+5.1}_{-2.2}$ (< 12.2)	$62.0^{+140.5}_{-60.6} \pm 2.5$ (< 336.1)	$5.0^{+5.7}_{-2.5} \pm 0.1$ (< 11.7)	1.0
4.377	522.7	1.05	0.25	$7.8^{+4.3}_{-3.2}$ (< 16.0)	$214.7^{+119.1}_{-88.7} \pm 8.8$ (< 443.3)	$9.4^{+2.6}_{-1.9} \pm 0.2$ (< 13.6)	2.8
4.396	507.8	1.05	0.25	$3.8^{+3.9}_{-3.8}$ (< 11.5)	$107.8^{+112.1}_{-109.3} \pm 4.4$ (< 330.7)	$6.7^{+3.5}_{-3.4} \pm 0.1$ (< 11.8)	1.6
4.416	1090.7	1.05	0.25	$7.0^{+5.4}_{-4.8}$ (< 18.4)	$93.6^{+72.2}_{-64.2} \pm 3.8$ (< 245.9)	$6.3^{+2.4}_{-2.2} \pm 0.1$ (< 10.2)	1.8
4.436	569.9	1.05	0.25	$8.3^{+5.2}_{-3.0}$ (< 17.9)	$208.6^{+131.5}_{-75.9} \pm 8.6$ (< 452.7)	$9.5^{+3.0}_{-1.7} \pm 0.2$ (< 14.0)	2.6
4.527	112.1	1.05	0.25	$0.5^{+2.6}_{-0.5}$ (< 5.2)	$65.0^{+337.9}_{-65.0} \pm 2.7$ (< 675.7)	$5.4^{+14.2}_{-2.7} \pm 0.1$ (< 17.6)	0.7
4.600	586.9	1.05	0.25	$0.5^{+4.2}_{-0.5}$ (< 8.8)	$12.5^{+105.3}_{-12.5} \pm 0.5$ (< 220.6)	$2.4^{+10.3}_{-1.2} \pm 0.1$ (< 10.3)	0.7
4.628	521.5	1.05	0.25	$0.5^{+3.5}_{-0.5}$ (< 7.3)	$14.2^{+99.2}_{-14.2} \pm 0.6$ (< 206.9)	$2.6^{+9.2}_{-1.3} \pm 0.1$ (< 10.0)	0.7
4.641	551.7	1.05	0.25	$5.8^{+4.1}_{-2.9}$ (< 13.6)	$154.3^{+110.0}_{-77.8} \pm 6.2$ (< 364.9)	$8.7^{+3.1}_{-2.2} \pm 0.2$ (< 13.4)	2.2
4.661	529.4	1.05	0.25	$2.0^{+3.2}_{-2.0}$ (< 8.6)	$54.5^{+87.2}_{-54.5} \pm 2.2$ (< 234.3)	$5.2^{+4.2}_{-2.6} \pm 0.1$ (< 10.8)	1.1
4.682	1667.4	1.05	0.25	$4.3^{+6.2}_{-4.2}$ (< 16.6)	$37.4^{+54.6}_{-37.0} \pm 1.5$ (< 146.3)	$4.3^{+3.2}_{-2.1} \pm 0.1$ (< 8.6)	1.3
4.740	163.9	1.05	0.25	$3.8^{+3.2}_{-2.1}$ (< 9.9)	$333.9^{+284.9}_{-187.0} \pm 13.4$ (< 881.4)	$13.2^{+5.6}_{-3.7} \pm 0.3$ (< 21.4)	2.0
4.750	366.6	1.05	0.25	$0.5^{+2.8}_{-0.5}$ (< 5.8)	$19.9^{+111.6}_{-19.9} \pm 0.8$ (< 231.1)	$3.2^{+9.1}_{-1.6} \pm 0.1$ (< 11.0)	0.7
4.781	511.5	1.06	0.25	$3.5^{+4.0}_{-2.3}$ (< 11.1)	$99.4^{+113.6}_{-65.3} \pm 4.0$ (< 315.3)	$7.3^{+4.2}_{-2.4} \pm 0.1$ (< 13.0)	1.5
4.918	207.8	1.06	0.25	$0.5^{+3.1}_{-0.5}$ (< 6.4)	$35.2^{+218.0}_{-35.2} \pm 1.4$ (< 450.0)	$4.5^{+14.0}_{-2.3} \pm 0.1$ (< 16.2)	0.7
4.951	159.3	1.06	0.25	$3.0^{+2.6}_{-1.9}$ (< 8.0)	$274.3^{+237.7}_{-173.7} \pm 11.0$ (< 731.5)	$12.7^{+5.5}_{-4.0} \pm 0.3$ (< 20.8)	1.9

Table 2. The CM energy ($\sqrt{s}$), the integrated luminosity ($\mathcal{L}$), the VP correction factor ($\frac{1}{|1-\prod|^2}$), the ISR correction factor and the detection efficiency ($\epsilon \cdot (1+\delta)$), the signal yield ($N_{\rm obs}$), the upper limit of signal yield at the 90% C.L. ($N^{\rm UL}$), the Born cross section (σ^B), the effective from factor ($|G_{\rm eff}(s)|$) and the statistical significance ($\mathcal{S}$). The first and second uncertainties for σ^B and $|G_{\rm eff}(s)|$ are statistical and systematic, respectively.

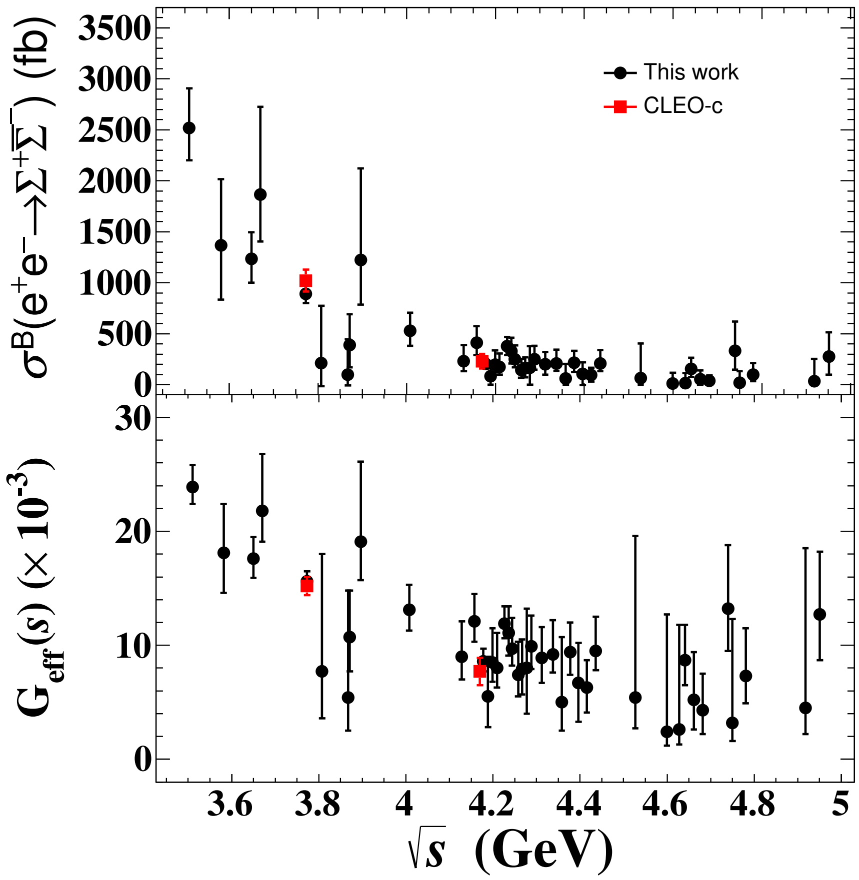

Figure 2. The measured Born cross section (top) and Σ^+ effective form factor (bottom) for $e^+e^- \to \Sigma^+\bar{\Sigma}^-$ versus CM energy, where the uncertainties include both the statistical and systematic ones.

5.2 $\Sigma^+(\bar{\Sigma}^-)$ reconstruction

The systematic uncertainty due to the $\Sigma^+(\bar{\Sigma}^-)$ reconstruction efficiency incorporating the tracking efficiencies, π^0 reconstruction, and $\Sigma^+(\bar{\Sigma}^-)$ mass windows, is estimated by the control sample of $\psi(3686) \to \Sigma^+\bar{\Sigma}^-$ with the same method as described in refs. [63–72]. The efficiency difference correlated with the angular distribution ($\cos\theta$) between data and MC is taken as the systematic uncertainty.

5.3 Background

The systematic uncertainty associated with the background, which is estimated based on the sidebands, is determined by shifting the sideband region inward or outward by 1σ. Since the number of events for each energy point is limited, all energy points are combined in the estimation. The maximum difference before and after moving the sideband region is taken as the systematic uncertainty.

$\sqrt{s}$ (GeV)	Luminosity	$\Sigma^+(\bar{\Sigma}^-)$ reconstruction	Background	AD	$\mathcal{B}$	ILS	Total
From 3.510 to 3.896	1.0	1.9	2.7	2.1	0.8	0.1	4.1
From 4.008 to 4.600	0.7	1.9	2.7	2.1	0.8	0.1	4.1
From 4.628 to 4.951	0.5	1.9	2.7	2.1	0.8	0.1	4.0

Table 3. Systematic uncertainties (in %) and their sources for each energy point on the Born cross section measurement. Here, AD denotes angular distribution, $\mathcal{B}$ denotes branching fraction, and ILS denotes input line shape.

5.4 Angular distribution

Since there are not enough events to determine the angular distribution for each energy point separately, a control sample with large statistics and a DIY model [44] with customizable angular distribution are used. With a large sample of $\psi(3770)$ events as the control sample, the angular distribution is obtained by a maximum likelihood fit to the helicity amplitude [73–75]. The DIY sample is initially generated with the central value of the fitting, and its efficiency is considered as the nominal result. Subsequently, two additional DIY samples are generated using the upper and lower limits of the fit uncertainty. The maximum difference in efficiency between them and the nominal one is taken as the systematic uncertainty.

5.5 Branching fractions

The uncertainty from the branching fraction of $\Sigma^+ \to p\pi^0$ is 0.58% from the PDG [45], and the uncertainty of the branching fraction of $\pi^0 \to \gamma\gamma$ is 0.03%. Combining with the branching fraction of the opposite side $\bar{\Sigma}^-$ decay, the systematic uncertainty from the branching fractions is 0.8%.

5.6 Input line shape

The systematic uncertainty of the input line shape is estimated by varying the central value of the nominal input line shape within $\pm 1\sigma$ of the statistical uncertainty, and the $\epsilon \cdot (1+\delta)$ value for each energy point is recalculated. This process is repeated 200 times, after which a Gaussian function is used to fit the $\epsilon \cdot (1+\delta)$ distribution. The width of the Gaussian function is taken as the corresponding systematic uncertainty.

5.7 Total systematic uncertainty

The various systematic uncertainties on the Born cross section measurement are summarized in table 3. Assuming all sources are independent, the total systematic uncertainty on the cross section measurement is determined by adding them in quadrature.

6 Fit to the dressed cross section

The potential resonances in the line shape of the cross section for the $e^+e^- \to \Sigma^+\bar{\Sigma}^-$ reaction are searched for by fitting the dressed cross section, $\sigma^{\text{dressed}} = \sigma^B/|1-\Pi|^2$ (including the VP effect), using the least χ^2 method:

$$\chi^2 = \Delta X^T V^{-1} \Delta X. \tag{6.1}$$

This is done considering the covariance matrix V and the vector of residuals ΔX between the measured and fitted cross sections. The covariance matrix incorporates both the correlated and uncorrelated uncertainties among different energy points. The systematic uncertainties associated with the luminosity, $\Sigma^+(\bar{\Sigma}^-)$ reconstruction, and branching fraction are assumed to be fully correlated among the CM energies, while the other systematic uncertainties are assumed to be uncorrelated.

Assuming the cross section of $e^+e^- \to \Sigma^+\bar{\Sigma}^-$ includes a resonance plus a continuum contribution, a fit to the dressed cross section with the coherent sum of a power-law (PL) function plus a Breit-Wigner (BW) function

$$\sigma^{\text{dressed}}(\sqrt{s}) = \left|\text{PL}(\sqrt{s}) + e^{i\phi}\text{BW}(\sqrt{s})\sqrt{\frac{P(\sqrt{s})}{P(M)}}\right|^2, \tag{6.2}$$

is applied. Here ϕ is the relative phase between the BW function

$$\text{BW}(\sqrt{s}) = \frac{\sqrt{12\pi\Gamma_{ee}\mathcal{B}\Gamma}}{s - M^2 + iM\Gamma}, \tag{6.3}$$

and the PL function

$$\text{PL}(\sqrt{s}) = \frac{c_0\sqrt{P(\sqrt{s})}}{\sqrt{s}^n}, \tag{6.4}$$

where c_0 and n are free fit parameters, $\sqrt{P(\sqrt{s})}$ is the two-body PHSP factor, the mass M and total width Γ are fixed to the assumed resonance with the PDG values [45], and $\Gamma_{ee}\mathcal{B}$ is the products of the electronic partial width and the branching fraction for the resonance decaying into the $\Sigma^+\bar{\Sigma}^-$ final state. Note that due to limited statistics, we only take into account the interference between the continuum contribution and each resonance, and no longer consider the interference between resonances. The parameters without a resonance are fitted to be ($c_0 = 2.3 \pm 0.8, n = 8.5 \pm 0.3$) with the goodness-of-fit $\chi^2/n.d.f = 31.2/(41 - 2)$, and the parameters including a resonance are summarized in table 4. Considering systematic uncertainties, the significance for each resonance is calculated by comparing the change of $\chi^2/n.d.f$ with and without the resonance. Charmonium(-like) states, $\psi(3770)$, $\psi(4040)$, $\psi(4160)$, $Y(4230)$, $Y(4360)$, $\psi(4415)$, $Y(4660)$, are all fitted separately by eq. (6.2), but no significant resonance is found. Thus, upper limits of the products of branching fraction and two-electronic partial width for these charmonium(-like) states decaying into the $\Sigma^+\bar{\Sigma}^-$ final state including the systematic uncertainty are determined at the 90% C.L. using a Bayesian approach [76]. Figure 3 shows the fit to the dressed cross section including a resonance [i.e. $\psi(3770)$, $\psi(4040)$, $\psi(4160)$, $Y(4230)$, $Y(4360)$, $\psi(4415)$ and $Y(4660)$] and without a resonance. Due to the quadratic form of the cross section like eq. (6.2), there are multiple solutions [77], which can be determined by scanning the parameters ϕ and $\Gamma_{ee}\mathcal{B}$, similar to the method used in ref. [25]. The fit results and their multiple solutions are summarized in table 4.

7 Summary

Using a total of 24.1 fb^{-1} of e^+e^- collision data above open-charm threshold collected with the BESIII detector at the BEPCII collider, the process $e^+e^- \to \Sigma^+\bar{\Sigma}^-$ is studied. The

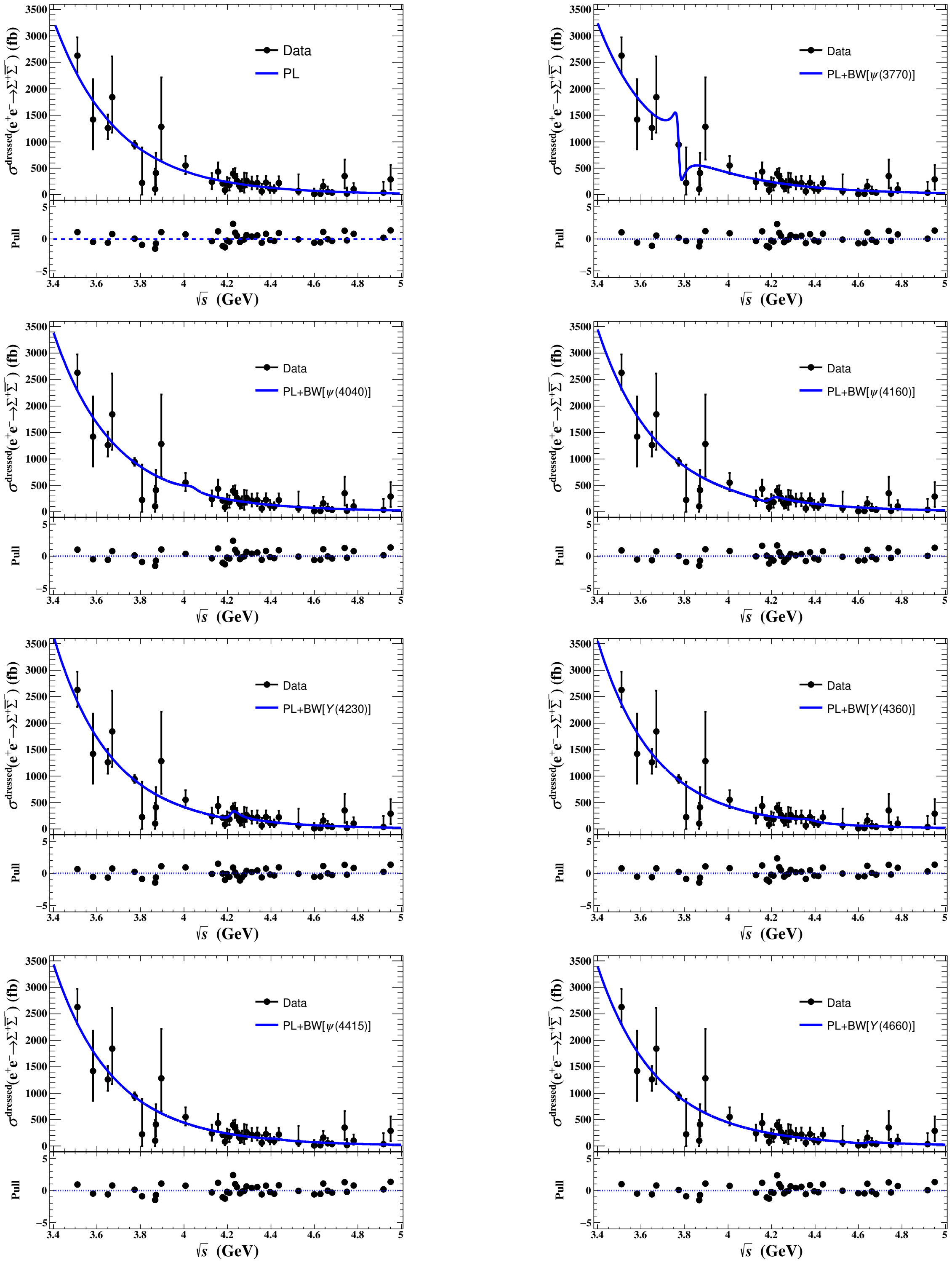

Figure 3. Fits to the dressed cross section at the CM energy from 3.510 to 4.951 GeV with the assumptions of a PL function only (upper left) and a power-law function plus a resonance ($\psi(3770)$, $\psi(4040)$, $\psi(4160)$, $Y(4230)$, $Y(4360)$, $\psi(4415)$, and $Y(4660)$). Dots with error bars are the dressed cross sections, and the solid lines show the fit results. The error bars represent the statistical and systematic uncertainties summed in quadrature.

Resonance parameters	Solution I	Solution II	$\chi^2/n.d.f$
$\phi_{\psi(3770)}$ (rad)	-2.6 ± 0.4	-2.0 ± 0.4	$28.8/(41-4)$
$\Gamma_{ee}\mathcal{B}_{\psi(3770)}(10^{-3}\text{eV})$	19.5 ± 29.1	73.8 ± 32.7 (< 101.5)	
$\phi_{\psi(4040)}$ (rad)	2.0 ± 0.6	-1.7 ± 0.1	$30.5/(41-4)$
$\Gamma_{ee}\mathcal{B}_{\psi(4040)}(10^{-3}\text{eV})$	0.2 ± 1.3	154.6 ± 29.0 (< 216.6)	
$\phi_{\psi(4160)}$ (rad)	-0.6 ± 0.5	-1.5 ± 0.1	$27.9/(41-4)$
$\Gamma_{ee}\mathcal{B}_{\psi(4160)}(10^{-3}\text{eV})$	0.8 ± 0.7	82.1 ± 5.6 (< 94.6)	
$\phi_{\psi(4230)}$ (rad)	0.4 ± 0.4	-1.5 ± 0.1	$26.5/(41-4)$
$\Gamma_{ee}\mathcal{B}_{\psi(4230)}(10^{-3}\text{eV})$	1.2 ± 0.8	60.1 ± 5.0 (< 72.4)	
$\phi_{\psi(4360)}$ (rad)	1.7 ± 0.7	-1.7 ± 0.1	$30.1/(41-4)$
$\Gamma_{ee}\mathcal{B}_{\psi(4360)}(10^{-3}\text{eV})$	0.5 ± 1.0	98.4 ± 10.4 (< 118.8)	
$\phi_{\psi(4415)}$ (rad)	0.8 ± 0.6	-1.6 ± 0.1	$30.5/(41-4)$
$\Gamma_{ee}\mathcal{B}_{\psi(4415)}(10^{-3}\text{eV})$	0.1 ± 0.5	47.7 ± 6.8 (< 62.1)	
$\phi_{\psi(4660)}$ (rad)	-0.3 ± 0.5	-1.5 ± 0.2	$30.6/(41-4)$
$\Gamma_{ee}\mathcal{B}_{\psi(4660)}(10^{-3}\text{eV})$	0.2 ± 1.6	31.1 ± 9.3 (< 49.6)	

Table 4. The fitted resonance parameters to the dressed cross section for the $e^+e^- \to \Sigma^+\bar{\Sigma}^-$ process with two solutions. The fit procedure includes both statistical and systematic uncertainties except for the CM energy calibration. The relative phase is given by ϕ.

Born cross sections and effective form factors are measured at 41 CM energies that range from 3.510 to 4.951 GeV. A fit to the dressed cross section of the $e^+e^- \to \Sigma^+\bar{\Sigma}^-$ reaction is performed, in which the line shape is described by a series of resonance hypotheses plus a continuum contribution, or only a continuum contribution. However, no obvious signal of $\psi(3770)$, $\psi(4040)$, $\psi(4160)$, $Y(4230)$, $Y(4360)$, $\psi(4415)$, or $Y(4660)$ is found, and upper limits for the products of branching fraction and di-electronic partial width at the 90% C.L. for these charmonium(-like) states decaying into the $\Sigma^+\bar{\Sigma}^-$ final state are determined.

Acknowledgments

The BESIII Collaboration thanks the staff of BEPCII and the IHEP computing center for their strong support. This work is supported in part by National Key R&D Program of China under Contracts Nos. 2020YFA0406400, 2020YFA0406300; National Natural Science Foundation of China (NSFC) under Contracts Nos. 12075107, 12247101, 11635010, 11735014, 11835012, 11935015, 11935016, 11935018, 11961141012, 12025502, 12035009, 12035013, 12061131003, 12192260, 12192261, 12192262, 12192263, 12192264, 12192265, 12221005, 12225509, 12235017; the 111 Project under Grant No. B20063; the Chinese Academy of Sciences (CAS) Large-Scale Scientific Facility Program; the CAS Center for Excellence in Particle Physics (CCEPP); Joint Large-Scale Scientific Facility Funds of the NSFC and CAS under Contract No. U1832207; CAS Key Research Program of Frontier Sciences under Contracts Nos. QYZDJ-SSW-SLH003, QYZDJ-SSW-SLH040; 100 Talents Program of CAS; The Institute of Nuclear and Particle Physics (INPAC) and Shanghai Key Laboratory for Particle Physics and Cosmology; European Union's Horizon 2020 research and innovation programme under Marie Sklodowska-

Curie grant agreement under Contract No. 894790; German Research Foundation DFG under Contracts Nos. 455635585, Collaborative Research Center CRC 1044, FOR5327, GRK 2149; Istituto Nazionale di Fisica Nucleare, Italy; Ministry of Development of Turkey under Contract No. DPT2006K-120470; National Research Foundation of Korea under Contract No. NRF-2022R1A2C1092335; National Science and Technology fund of Mongolia; National Science Research and Innovation Fund (NSRF) via the Program Management Unit for Human Resources & Institutional Development, Research and Innovation of Thailand under Contract No. B16F640076; Polish National Science Centre under Contract No. 2019/35/O/ST2/02907; The Swedish Research Council; U. S. Department of Energy under Contract No. DE-FG02-05ER41374

References

[1] T. Barnes, S. Godfrey and E.S. Swanson, *Higher charmonia*, *Phys. Rev. D* **72** (2005) 054026 [`hep-ph/0505002`] [INSPIRE].

[2] N. Brambilla et al., *Heavy quarkonium: progress, puzzles, and opportunities*, *Eur. Phys. J. C* **71** (2011) 1534 [`arXiv:1010.5827`] [INSPIRE].

[3] BES collaboration, *Measurements of the cross-section for $e^+e^- \to$ hadrons at center-of-mass energies from* 2 *GeV to* 5 *GeV*, *Phys. Rev. Lett.* **88** (2002) 101802 [`hep-ex/0102003`] [INSPIRE].

[4] BaBar collaboration, *Observation of a broad structure in the $\pi^+\pi^- J/\psi$ mass spectrum around* 4.26 *GeV/c^2*, *Phys. Rev. Lett.* **95** (2005) 142001 [`hep-ex/0506081`] [INSPIRE].

[5] BaBar collaboration, *Evidence of a broad structure at an invariant mass of* 4.32 *GeV/c^2 in the reaction $e^+e^- \to \pi^+\pi^-\psi(2S)$ measured at BaBar*, *Phys. Rev. Lett.* **98** (2007) 212001 [`hep-ex/0610057`] [INSPIRE].

[6] Belle collaboration, *Observation of two resonant structures in $e^+e^- \to \pi^+\pi^-\psi(2S)$ via initial state radiation at Belle*, *Phys. Rev. Lett.* **99** (2007) 142002 [`arXiv:0707.3699`] [INSPIRE].

[7] Belle collaboration, *Measurement of $e^+e^- \to \pi^+\pi^- J/\psi$ cross-section via initial state radiation at Belle*, *Phys. Rev. Lett.* **99** (2007) 182004 [`arXiv:0707.2541`] [INSPIRE].

[8] Belle collaboration, *Observation of a near-threshold enhancement in the $e^+e^- \to \Lambda_c^+\Lambda_c^-$ cross section using initial-state radiation*, *Phys. Rev. Lett.* **101** (2008) 172001 [`arXiv:0807.4458`] [INSPIRE].

[9] BaBar collaboration, *Study of the reaction $e^+e^- \to J/\psi\pi^+\pi^-$ via initial-state radiation at BaBar*, *Phys. Rev. D* **86** (2012) 051102 [`arXiv:1204.2158`] [INSPIRE].

[10] Belle collaboration, *Study of $e^+e^- \to \pi^+\pi^- J/\psi$ and observation of a charged charmonium-like state at Belle*, *Phys. Rev. Lett.* **110** (2013) 252002 [*Erratum ibid.* **111** (2013) 019901] [`arXiv:1304.0121`] [INSPIRE].

[11] BaBar collaboration, *Study of the reaction $e^+e^- \to \psi(2S)\pi^-\pi^-$ via initial-state radiation at BaBar*, *Phys. Rev. D* **89** (2014) 111103 [`arXiv:1211.6271`] [INSPIRE].

[12] Belle collaboration, *Measurement of $e^+e^- \to \pi^+\pi^-\psi(2S)$ via initial state radiation at Belle*, *Phys. Rev. D* **91** (2015) 112007 [`arXiv:1410.7641`] [INSPIRE].

[13] CLEO collaboration, *Charmonium decays of $Y(4260)$, $\psi(4160)$ and $\psi(4040)$*, *Phys. Rev. Lett.* **96** (2006) 162003 [`hep-ex/0602034`] [INSPIRE].

[14] BESIII collaboration, *Study of $e^+e^- \to \omega\chi_{cJ}$ at center-of-mass energies from 4.21 to 4.42 GeV*, *Phys. Rev. Lett.* **114** (2015) 092003 [`arXiv:1410.6538`] [INSPIRE].

[15] BESIII collaboration, *Observation of three charmoniumlike states with $J^{PC} = 1^{--}$ in $e^+e^- \to D^{*0}D^{*-}\pi^+$*, *Phys. Rev. Lett.* **130** (2023) 121901 [`arXiv:2301.07321`] [INSPIRE].

[16] F.E. Close and P.R. Page, *Gluonic charmonium resonances at BaBar and BELLE?*, *Phys. Lett. B* **628** (2005) 215 [`hep-ph/0507199`] [INSPIRE].

[17] R.A. Briceno et al., *Issues and opportunities in exotic hadrons*, *Chin. Phys. C* **40** (2016) 042001 [`arXiv:1511.06779`] [INSPIRE].

[18] H.-X. Chen, W. Chen, X. Liu and S.-L. Zhu, *The hidden-charm pentaquark and tetraquark states*, *Phys. Rept.* **639** (2016) 1 [`arXiv:1601.02092`] [INSPIRE].

[19] J.-Z. Wang, D.-Y. Chen, X. Liu and T. Matsuki, *Constructing J/ψ family with updated data of charmoniumlike Y states*, *Phys. Rev. D* **99** (2019) 114003 [`arXiv:1903.07115`] [INSPIRE].

[20] R.-Q. Qian, Q. Huang and X. Liu, *Predicted $\Lambda\bar{\Lambda}$ and $\Xi^-\bar{\Xi}^+$ decay modes of the charmoniumlike $Y(4230)$*, *Phys. Lett. B* **833** (2022) 137292 [`arXiv:2111.13821`] [INSPIRE].

[21] B. Yan, C. Chen and J.-J. Xie, *Σ and Ξ electromagnetic form factors in the extended vector meson dominance model*, *Phys. Rev. D* **107** (2023) 076008 [`arXiv:2301.00976`] [INSPIRE].

[22] J.-P. Dai, X. Cao and H. Lenske, *Data driven isospin analysis of timelike octet baryons electromagnetic form factors and charmonium decay into baryon-anti-baryon*, *Phys. Lett. B* **846** (2023) 138192 [`arXiv:2304.04913`] [INSPIRE].

[23] J.-Z. Wang and X. Liu, *Identifying a characterized energy level structure of higher charmonium well matched to the peak structures in $e^+e^- \to \pi^+D^0D^{*-}$*, *Phys. Lett. B* **849** (2024) 138456 [`arXiv:2306.14695`] [INSPIRE].

[24] BESIII collaboration, *Search for baryonic decays of $\psi(3770)$ and $\psi(4040)$*, *Phys. Rev. D* **87** (2013) 112011 [`arXiv:1305.1782`] [INSPIRE].

[25] BESIII collaboration, *Measurement of the cross section for $e^+e^- \to \Lambda\bar{\Lambda}$ and evidence of the decay $\psi(3770) \to \Lambda\bar{\Lambda}$*, *Phys. Rev. D* **104** (2021) L091104 [`arXiv:2108.02410`] [INSPIRE].

[26] BESIII collaboration, *Measurement of the cross section for $e^+e^- \to \Xi^-\bar{\Xi}^+$ and observation of an excited Ξ baryon*, *Phys. Rev. Lett.* **124** (2020) 032002 [`arXiv:1910.04921`] [INSPIRE].

[27] BESIII collaboration, *Measurement of the cross section of $e^+e^- \to \Xi^-\bar{\Xi}^+$ at center-of-mass energies between 3.510 and 4.843 GeV*, *JHEP* **11** (2023) 228 [`arXiv:2309.04215`] [INSPIRE].

[28] BESIII collaboration, *Precision measurement of the $e^+e^- \to \Lambda_c^+\bar{\Lambda}_c^-$ cross section near threshold*, *Phys. Rev. Lett.* **120** (2018) 132001 [`arXiv:1710.00150`] [INSPIRE].

[29] BESIII collaboration, *Study of baryon pair production at BESIII*, *PoS* **CHARM2020** (2021) 026 [INSPIRE].

[30] X. Wang, *Hyperon pair production at BESIII*, *Rev. Mex. Fis. Suppl.* **3** (2022) 0308074 [INSPIRE].

[31] H. Liu, J. Zhang and X. Wang, *CP asymmetry in the Ξ hyperon sector*, *Symmetry* **15** (2023) 214 [INSPIRE].

[32] BESIII collaboration, *Design and construction of the BESIII detector*, *Nucl. Instrum. Meth. A* **614** (2010) 345 [`arXiv:0911.4960`] [INSPIRE].

[33] C. Yu et al., *BEPCII performance and beam dynamics studies on luminosity*, in the proceedings of the 7th *International Particle Accelerator Conference*, (2016) [`DOI:10.18429/JACoW-IPAC2016-TUYA01`] [INSPIRE].

[34] BESIII collaboration, *Future physics programme of BESIII*, *Chin. Phys. C* **44** (2020) 040001 [`arXiv:1912.05983`] [INSPIRE].

[35] J. Lu, Y. Xiao and X. Ji, *Online monitoring of the center-of-mass energy from real data at BESIII*, *Radiat. Detect. Technol. Methods* **4** (2020) 337.

[36] J.-W. Zhang et al., *Suppression of top-up injection backgrounds with offline event filter in the BESIII experiment*, *Radiat. Detect. Technol. Methods* **6** (2022) 289 [INSPIRE].

[37] X. Li et al., *Study of MRPC technology for BESIII endcap-TOF upgrade*, *Radiat. Detect. Technol. Methods* **1** (2017) 13 [INSPIRE].

[38] Y.-X. Guo et al., *The study of time calibration for upgraded end cap TOF of BESIII*, *Radiat. Detect. Technol. Methods* **1** (2017) 15 [INSPIRE].

[39] P. Cao et al., *Design and construction of the new BESIII endcap time-of-flight system with MRPC technology*, *Nucl. Instrum. Meth. A* **953** (2020) 163053 [INSPIRE].

[40] GEANT4 collaboration, *GEANT4 — a simulation toolkit*, *Nucl. Instrum. Meth. A* **506** (2003) 250 [INSPIRE].

[41] K.-X. Huang et al., *Method for detector description transformation to unity and application in BESIII*, *Nucl. Sci. Tech.* **33** (2022) 142 [`arXiv:2206.10117`] [INSPIRE].

[42] S. Jadach, B.F.L. Ward and Z. Was, *Coherent exclusive exponentiation for precision Monte Carlo calculations*, *Phys. Rev. D* **63** (2001) 113009 [`hep-ph/0006359`] [INSPIRE].

[43] D.J. Lange, *The EvtGen particle decay simulation package*, *Nucl. Instrum. Meth. A* **462** (2001) 152 [INSPIRE].

[44] R.-G. Ping, *Event generators at BESIII*, *Chin. Phys. C* **32** (2008) 599 [INSPIRE].

[45] PARTICLE DATA GROUP collaboration, *Review of particle physics*, *PTEP* **2022** (2022) 083C01 [INSPIRE].

[46] M. Oreglia, *A study of the reactions* $\psi' \to \gamma\gamma\psi$, SLAC-0236 (1980) [INSPIRE].

[47] G.J. Feldman and R.D. Cousins, *A unified approach to the classical statistical analysis of small signals*, *Phys. Rev. D* **57** (1998) 3873 [`physics/9711021`] [INSPIRE].

[48] Y.-S. Zhu, *On statistical significance of signal*, *HEPNP* **30** (2006) 331 [`arXiv:0812.2708`] [INSPIRE].

[49] J. Lundberg, J. Conrad, W. Rolke and A. Lopez, *Limits, discovery and cut optimization for a Poisson process with uncertainty in background and signal efficiency: TRolke* 2.0, *Comput. Phys. Commun.* **181** (2010) 683 [`arXiv:0907.3450`] [INSPIRE].

[50] E.A. Kuraev and V.S. Fadin, *On radiative corrections to* e^+e^- *single photon annihilation at high-energy*, *Sov. J. Nucl. Phys.* **41** (1985) 466 [INSPIRE].

[51] F. Jegerlehner and R. Szafron, $\rho^0 - \gamma$ *mixing in the neutral channel pion form factor* F_π^e *and its role in comparing* e^+e^- *with* τ *spectral functions*, *Eur. Phys. J. C* **71** (2011) 1632 [`arXiv:1101.2872`] [INSPIRE].

[52] W. Sun et al., *An iterative weighting method to apply ISR correction to* e^+e^- *hadronic cross-section measurements*, *Front. Phys. (Beijing)* **16** (2021) 64501 [`arXiv:2011.07889`] [INSPIRE].

[53] R. Baldini, S. Pacetti, A. Zallo and A. Zichichi, *Unexpected features of* $e^+e^- \to p\bar{p}$ *and* $e^+e^- \to \Lambda\bar{\Lambda}$ *cross sections near threshold*, *Eur. Phys. J. A* **39** (2009) 315 [`arXiv:0711.1725`] [INSPIRE].

[54] A.B. Arbuzov and T.V. Kopylova, *On relativization of the Sommerfeld-Gamow-Sakharov factor*, *JHEP* **04** (2012) 009 [`arXiv:1111.4308`] [INSPIRE].

[55] A. Sommerfeld, *Über die Beugung und Bremsung der Elektronen* (in German), *Annalen Phys.* **403** (1931) 257 [INSPIRE].

[56] C. Tzara, *Effect of the Coulomb potential on the* π^- *photoproduction*, *Nucl. Phys. B* **18** (1970) 246 [INSPIRE].

[57] A.D. Sakharov, *Interaction of an electron and positron in pair production*, *Zh. Eksp. Teor. Fiz.* **18** (1948) 631 [INSPIRE].

[58] X. Wang and G. Huang, *Electromagnetic form factor of doubly-strange hyperon*, *Symmetry* **14** (2022) 65 [INSPIRE].

[59] S. Dobbs et al., *Hyperon form factors & diquark correlations*, *Phys. Rev. D* **96** (2017) 092004 [`arXiv:1708.09377`] [INSPIRE].

[60] BESIII collaboration, *Precision measurement of the integrated luminosity of the data taken by BESIII at center of mass energies between* 3.810 *GeV and* 4.600 *GeV*, *Chin. Phys. C* **39** (2015) 093001 [`arXiv:1503.03408`] [INSPIRE].

[61] BESIII collaboration, *Measurement of integrated luminosities at BESIII for data samples at center-of-mass energies between* 4.0 *and* 4.6 *GeV*, *Chin. Phys. C* **46** (2022) 113002 [`arXiv:2203.03133`] [INSPIRE].

[62] BESIII collaboration, *Luminosities and energies of* e^+e^- *collision data taken between* 4.61 *GeV and* 4.95 *GeV at BESIII*, *Chin. Phys. C* **46** (2022) 113003 [`arXiv:2205.04809`] [INSPIRE].

[63] BESIII collaboration, *Study of* ψ *decays to the* $\Xi^-\bar{\Xi}^+$ *and* $\Sigma(1385)^{\mp}\bar{\Sigma}(1385)^{\pm}$ *final states*, *Phys. Rev. D* **93** (2016) 072003 [`arXiv:1602.06754`] [INSPIRE].

[64] BESIII collaboration, *Study of* J/ψ *and* $\psi(3686) \to \Sigma(1385)^0\bar{\Sigma}(1385)^0$ *and* $\Xi^0\bar{\Xi}^0$, *Phys. Lett. B* **770** (2017) 217 [`arXiv:1612.08664`] [INSPIRE].

[65] BESIII collaboration, *Observation of* $\psi(3686) \to \Xi(1530)^-\bar{\Xi}(1530)^+$ *and* $\Xi(1530)^-\bar{\Xi}^+$, *Phys. Rev. D* **100** (2019) 051101 [`arXiv:1907.13041`] [INSPIRE].

[66] BESIII collaboration, *Measurement of cross section for* $e^+e^- \to \Xi^-\bar{\Xi}^+$ *near threshold at BESIII*, *Phys. Rev. D* **103** (2021) 012005 [`arXiv:2010.08320`] [INSPIRE].

[67] BESIII collaboration, *Measurement of cross section for* $e^+e^- \to \Xi^0\bar{\Xi}^0$ *near threshold*, *Phys. Lett. B* **820** (2021) 136557 [`arXiv:2105.14657`] [INSPIRE].

[68] BESIII collaboration, *Observation of* $\psi(3686) \to \Xi(1530)^0\bar{\Xi}(1530)^0$ *and* $\Xi(1530)^0\bar{\Xi}^0$, *Phys. Rev. D* **104** (2021) 092012 [`arXiv:2109.06621`] [INSPIRE].

[69] BESIII collaboration, *Study of the processes* $\chi_{cJ} \to \Xi^-\bar{\Xi}^+$ *and* $\Xi^0\bar{\Xi}^0$, *JHEP* **06** (2022) 074 [`arXiv:2202.08058`] [INSPIRE].

[70] BESIII collaboration, *Observation of* Ξ^- *hyperon transverse polarization in* $\psi(3686) \to \Xi^-\bar{\Xi}^+$, *Phys. Rev. D* **106** (2022) L091101 [`arXiv:2206.10900`] [INSPIRE].

[71] BESIII collaboration, *First simultaneous measurement of* Ξ^0 *and* $\bar{\Xi}^0$ *asymmetry parameters in* $\psi(3686)$ *decay*, *Phys. Rev. D* **108** (2023) L011101 [`arXiv:2302.09767`] [INSPIRE].

[72] BESIII collaboration, *Study of $e^+e^- \to \Omega^-\bar{\Omega}^+$ at center-of-mass energies from* 3.49 *to* 3.67 *GeV*, *Phys. Rev. D* **107** (2023) 052003 [`arXiv:2212.03693`] [INSPIRE].

[73] G. Fäldt and A. Kupsc, *Hadronic structure functions in the $e^+e^- \to \bar{\Lambda}\Lambda$ reaction*, *Phys. Lett. B* **772** (2017) 16 [`arXiv:1702.07288`] [INSPIRE].

[74] BESIII collaboration, *Measurement of Λ baryon polarization in $e^+e^- \to \Lambda\bar{\Lambda}$ at $\sqrt{s} = 3.773$ GeV*, *Phys. Rev. D* **105** (2022) L011101 [`arXiv:2111.11742`] [INSPIRE].

[75] BESIII collaboration, *Measurement of Λ transverse polarization in e^+e^- collisions at $\sqrt{s} = 3.68$–3.71 GeV*, *JHEP* **10** (2023) 081 [*Erratum ibid.* **12** (2023) 080] [`arXiv:2303.00271`] [INSPIRE].

[76] Y.-S. Zhu, *Bayesian credible interval construction for Poisson statistics*, *Chin. Phys. C* **32** (2008) 363 [`arXiv:0812.2705`] [INSPIRE].

[77] Y. Bai and D.-Y. Chen, *General mathematical analysis on multiple solutions of interfering resonances combinations*, *Phys. Rev. D* **99** (2019) 072007 [`arXiv:1901.01394`] [INSPIRE].

The BESIII collaboration

M. Ablikim[1], M.N. Achasov[4,c], P. Adlarson[75], O. Afedulidis[3], X.C. Ai[80], R. Aliberti[35], A. Amoroso[74A,74C], Q. An[71,58,a], Y. Bai[57], O. Bakina[36], I. Balossino[29A], Y. Ban[46,h], H.-R. Bao[63], V. Batozskaya[1,44], K. Begzsuren[32], N. Berger[35], M. Berlowski[44], M. Bertani[28A], D. Bettoni[29A], F. Bianchi[74A,74C], E. Bianco[74A,74C], A. Bortone[74A,74C], I. Boyko[36], R.A. Briere[5], A. Brueggemann[68], H. Cai[76], X. Cai[1,58], A. Calcaterra[28A], G.F. Cao[1,63], N. Cao[1,63], S.A. Cetin[62A], J.F. Chang[1,58], G.R. Che[43], G. Chelkov[36,b], C. Chen[43], C.H. Chen[9], Chao Chen[55], G. Chen[1], H.S. Chen[1,63], H.Y. Chen[20], M.L. Chen[1,58,63], S.J. Chen[42], S.L. Chen[45], S.M. Chen[61], T. Chen[1,63], X.R. Chen[31,63], X.T. Chen[1,63], Y.B. Chen[1,58], Y.Q. Chen[34], Z.J. Chen[25,i], Z.Y. Chen[1,63], S.K. Choi[10], G. Cibinetto[29A], F. Cossio[74C], J.J. Cui[50], H.L. Dai[1,58], J.P. Dai[78], A. Dbeyssi[18], R. E. de Boer[3], D. Dedovich[36], C.Q. Deng[72], Z.Y. Deng[1], A. Denig[35], I. Denysenko[36], M. Destefanis[74A,74C], F. De Mori[74A,74C], B. Ding[66,1], X.X. Ding[46,h], Y. Ding[34], Y. Ding[40], J. Dong[1,58], L.Y. Dong[1,63], M.Y. Dong[1,58,63], X. Dong[76], M.C. Du[1], S.X. Du[80], Z.H. Duan[42], P. Egorov[36,b], Y.H. Fan[45], J. Fang[59], J. Fang[1,58], S.S. Fang[1,63], W.X. Fang[1], Y. Fang[1], Y.Q. Fang[1,58], R. Farinelli[29A], L. Fava[74B,74C], F. Feldbauer[3], G. Felici[28A], C.Q. Feng[71,58], J.H. Feng[59], Y.T. Feng[71,58], M. Fritsch[3], C.D. Fu[1], J.L. Fu[63], Y.W. Fu[1,63], H. Gao[63], X.B. Gao[41], Y.N. Gao[46,h], Yang Gao[71,58], S. Garbolino[74C], I. Garzia[29A,29B], L. Ge[80], P.T. Ge[76], Z.W. Ge[42], C. Geng[59], E.M. Gersabeck[67], A. Gilman[69], K. Goetzen[13], L. Gong[40], W.X. Gong[1,58], W. Gradl[35], S. Gramigna[29A,29B], M. Greco[74A,74C], M.H. Gu[1,58], Y.T. Gu[15], C.Y. Guan[1,63], Z.L. Guan[22], A.Q. Guo[31,63], L.B. Guo[41], M.J. Guo[50], R.P. Guo[49], Y.P. Guo[12,g], A. Guskov[36,b], J. Gutierrez[27], K.L. Han[63], T.T. Han[1], X.Q. Hao[19], F.A. Harris[65], K.K. He[55], K.L. He[1,63], F.H. Heinsius[3], C.H. Heinz[35], Y.K. Heng[1,58,63], C. Herold[60], T. Holtmann[3], P.C. Hong[34], G.Y. Hou[1,63], X.T. Hou[1,63], Y.R. Hou[63], Z.L. Hou[1], B.Y. Hu[59], H.M. Hu[1,63], J.F. Hu[56,j], S.L. Hu[12,g], T. Hu[1,58,63], Y. Hu[1], G.S. Huang[71,58], K.X. Huang[59], L.Q. Huang[31,63], X.T. Huang[50], Y.P. Huang[1], T. Hussain[73], F. Hölzken[3], N Hüsken[27,35], N. in der Wiesche[68], J. Jackson[27], S. Janchiv[32], J.H. Jeong[10], Q. Ji[1], Q.P. Ji[19], W. Ji[1,63], X.B. Ji[1,63], X.L. Ji[1,58], Y.Y. Ji[50], X.Q. Jia[50], Z.K. Jia[71,58], D. Jiang[1,63], H.B. Jiang[76], P.C. Jiang[46,h], S.S. Jiang[39], T.J. Jiang[16], X.S. Jiang[1,58,63], Y. Jiang[63], J.B. Jiao[50], J.K. Jiao[34], Z. Jiao[23], S. Jin[42], Y. Jin[66], M.Q. Jing[1,63], X.M. Jing[63], T. Johansson[75], S. Kabana[33], N. Kalantar-Nayestanaki[64], X.L. Kang[9], X.S. Kang[40], M. Kavatsyuk[64], B.C. Ke[80], V. Khachatryan[27], A. Khoukaz[68], R. Kiuchi[1], O.B. Kolcu[62A], B. Kopf[3], M. Kuessner[3], X. Kui[1,63], N. Kumar[26], A. Kupsc[44,75], W. Kühn[37], J.J. Lane[67], P. Larin[18], L. Lavezzi[74A,74C], T.T. Lei[71,58], Z.H. Lei[71,58], M. Lellmann[35], T. Lenz[35], C. Li[43], C. Li[47], C.H. Li[39], Cheng Li[71,58], D.M. Li[80], F. Li[1,58], G. Li[1], H.B. Li[1,63], H.J. Li[19], H.N. Li[56,j], Hui Li[43], J.R. Li[61], J.S. Li[59], Ke Li[1], L. J Li[1,63], L.K. Li[1], Lei Li[48], M.H. Li[43], P.R. Li[38,l], Q.M. Li[1,63], Q.X. Li[50], R. Li[17,31], S.X. Li[12], T. Li[50], W.D. Li[1,63], W.G. Li[1,a], X. Li[1,63], X.H. Li[71,58], X.L. Li[50], X.Z. Li[59], Xiaoyu Li[1,63], Y.G. Li[46,h], Z.J. Li[59], Z.X. Li[15], C. Liang[42], H. Liang[71,58], H. Liang[1,63], Y.F. Liang[54], Y.T. Liang[31,63], G.R. Liao[14], L.Z. Liao[50], J. Libby[26], A. Limphirat[60], C.C. Lin[55], D.X. Lin[31,63], T. Lin[1], B.J. Liu[1], B.X. Liu[76], C. Liu[34], C.X. Liu[1], F.H. Liu[53], Fang Liu[1], Feng Liu[6], G.M. Liu[56,j], H. Liu[38,k,l], H.B. Liu[15], H.M. Liu[1,63], Huanhuan Liu[1], Huihui Liu[21], J.B. Liu[71,58], J.Y. Liu[1,63], K. Liu[38,k,l], K.Y. Liu[40], Ke Liu[22], L. Liu[71,58], L.C. Liu[43], Lu Liu[43], M.H. Liu[12,g], P.L. Liu[1], Q. Liu[63], S.B. Liu[71,58], T. Liu[12,g], W.K. Liu[43], W.M. Liu[71,58], X. Liu[38,k,l], X. Liu[39], Y. Liu[80], Y. Liu[38,k,l], Y.B. Liu[43], Z.A. Liu[1,58,63], Z.D. Liu[9], Z.Q. Liu[50], X.C. Lou[1,58,63], F.X. Lu[59], H.J. Lu[23], J.G. Lu[1,58], X.L. Lu[1], Y. Lu[7], Y.P. Lu[1,58], Z.H. Lu[1,63], C.L. Luo[41], M.X. Luo[79], T. Luo[12,g], X.L. Luo[1,58], X.R. Lyu[63], Y.F. Lyu[43], F.C. Ma[40], H. Ma[78], H.L. Ma[1], J.L. Ma[1,63], L.L. Ma[50], M.M. Ma[1,63], Q.M. Ma[1], R.Q. Ma[1,63], X.T. Ma[1,63], X.Y. Ma[1,58], Y. Ma[46,h], Y.M. Ma[31], F.E. Maas[18], M. Maggiora[74A,74C], S. Malde[69], Y.J. Mao[46,h], Z.P. Mao[1], S. Marcello[74A,74C], Z.X. Meng[66], J.G. Messchendorp[13,64], G. Mezzadri[29A], H. Miao[1,63], T.J. Min[42], R.E. Mitchell[27], X.H. Mo[1,58,63], B. Moses[27], N. Yu. Muchnoi[4,c], J. Muskalla[35], Y. Nefedov[36], F. Nerling[18,e], L.S. Nie[20], I.B. Nikolaev[4,c], Z. Ning[1,58], S. Nisar[11,m], Q.L. Niu[38,k,l], W.D. Niu[55], Y. Niu [50], S.L. Olsen[63], Q. Ouyang[1,58,63], S. Pacetti[28B,28C], X. Pan[55], Y. Pan[57], A. Pathak[34], P. Patteri[28A], Y.P. Pei[71,58], M. Pelizaeus[3], H.P. Peng[71,58], Y.Y. Peng[38,k,l], K. Peters[13,e], J.L. Ping[41], R.G. Ping[1,63], S. Plura[35], V. Prasad[33], F.Z. Qi[1], H. Qi[71,58], H.R. Qi[61], M. Qi[42], T.Y. Qi[12,g], S. Qian[1,58], W.B. Qian[63], C.F. Qiao[63], X.K. Qiao[80], J.J. Qin[72], L.Q. Qin[14], L.Y. Qin[71,58], X.S. Qin[50], Z.H. Qin[1,58], J.F. Qiu[1], Z.H. Qu[72], C.F. Redmer[35], K.J. Ren[39], A. Rivetti[74C], M. Rolo[74C], G. Rong[1,63], Ch. Rosner[18], S.N. Ruan[43], N. Salone[44], A. Sarantsev[36,d], Y. Schelhaas[35], K. Schoenning[75], M. Scodeggio[29A], K.Y. Shan[12,g], W. Shan[24], X.Y. Shan[71,58], Z. J Shang[38,k,l], J.F. Shangguan[55], L.G. Shao[1,63], M. Shao[71,58], C.P. Shen[12,g], H.F. Shen[1,8], W.H. Shen[63], X.Y. Shen[1,63], B.A. Shi[63], H. Shi[71,58], H.C. Shi[71,58], J.L. Shi[12,g], J.Y. Shi[1], Q.Q. Shi[55], S.Y. Shi[72], X. Shi[1,58], J.J. Song[19], T.Z. Song[59], W.M. Song[34,1], Y. J. Song[12,g], Y.X. Song[46,h,n], S. Sosio[74A,74C], S. Spataro[74A,74C], F. Stieler[35], Y.J. Su[63], G.B. Sun[76], G.X. Sun[1], H. Sun[63], H.K. Sun[1], J.F. Sun[19], K. Sun[61], L. Sun[76], S.S. Sun[1,63], T. Sun[51,f], W.Y. Sun[34], Y. Sun[9], Y.J. Sun[71,58], Y.Z. Sun[1], Z.Q. Sun[1,63], Z.T. Sun[50], C.J. Tang[54], G.Y. Tang[1], J. Tang[59], Y.A. Tang[76], L.Y. Tao[72], Q.T. Tao[25,i], M. Tat[69], J.X. Teng[71,58], V. Thoren[75], W.H. Tian[59], Y. Tian[31,63], Z.F. Tian[76], I. Uman[62B], Y. Wan[55], S.J. Wang[50], B. Wang[1], B.L. Wang[63], Bo Wang[71,58], D.Y. Wang[46,h], F. Wang[72], H.J. Wang[38,k,l], J.J. Wang[76], J.P. Wang [50], K. Wang[1,58], L.L. Wang[1], M. Wang[50], Meng Wang[1,63], N.Y. Wang[63], S. Wang[12,g], S. Wang[38,k,l], T. Wang[12,g], T.J. Wang[43], W. Wang[72], W. Wang[59], W.P. Wang[35,71,o], X. Wang[46,h], X.F. Wang[38,k,l], X.J. Wang[39], X.L. Wang[12,g], X.N. Wang[1], Y. Wang[61], Y.D. Wang[45], Y.F. Wang[1,58,63], Y.L. Wang[19], Y.N. Wang[45], Y.Q. Wang[1], Yaqian Wang[17], Yi Wang[61], Z. Wang[1,58], Z.L. Wang[72], Z.Y. Wang[1,63], Ziyi Wang[63], D.H. Wei[14], F. Weidner[68], S.P. Wen[1], Y.R. Wen[39], U. Wiedner[3], G. Wilkinson[69], M. Wolke[75], L. Wollenberg[3], C. Wu[39], J.F. Wu[1,8], L.H. Wu[1], L.J. Wu[1,63], X. Wu[12,g], X.H. Wu[34], Y. Wu[71,58], Y.H. Wu[55], Y.J. Wu[31], Z. Wu[1,58], L. Xia[71,58], X.M. Xian[39], B.H. Xiang[1,63], T. Xiang[46,h], D. Xiao[38,k,l], G.Y. Xiao[42], S.Y. Xiao[1], Y. L. Xiao[12,g], Z.J. Xiao[41], C. Xie[42], X.H. Xie[46,h], Y. Xie[50], Y.G. Xie[1,58], Y.H. Xie[6], Z.P. Xie[71,58], T.Y. Xing[1,63], C.F. Xu[1,63], C.J. Xu[59], G.F. Xu[1], H.Y. Xu[66], M. Xu[71,58], Q.J. Xu[16], Q.N. Xu[30], W. Xu[1], W.L. Xu[66], X.P. Xu[55], Y.C. Xu[77], Z.P. Xu[42], Z.S. Xu[63], F. Yan[12,g], L. Yan[12,g], W.B. Yan[71,58], W.C. Yan[80], X.Q. Yan[1], H.J. Yang[51,f], H.L. Yang[34], H.X. Yang[1], Tao Yang[1], Y. Yang[12,g], Y.F. Yang[43], Y.X. Yang[1,63], Yifan Yang[1,63], Z.W. Yang[38,k,l], Z.P. Yao[50], M. Ye[1,58], M.H. Ye[8], J.H. Yin[1], Z.Y. You[59], B.X. Yu[1,58,63], C.X. Yu[43], G. Yu[1,63], J.S. Yu[25,i], T. Yu[72], X.D. Yu[46,h], Y.C. Yu[80], C.Z. Yuan[1,63], J. Yuan[34], L. Yuan[2], S.C. Yuan[1], Y. Yuan[1,63], Y.J. Yuan[45], Z.Y. Yuan[59], C.X. Yue[39], A.A. Zafar[73], F.R. Zeng[50], S.H. Zeng[72], X. Zeng[12,g], Y. Zeng[25,i], Y.J. Zeng[59], X.Y. Zhai[34], Y.C. Zhai[50], Y.H. Zhan[59], A.Q. Zhang[1,63], B.L. Zhang[1,63], B.X. Zhang[1], D.H. Zhang[43], G.Y. Zhang[19], H. Zhang[80], H. Zhang[71,58], H.C. Zhang[1,58,63], H.H. Zhang[34], H.H. Zhang[59], H.Q. Zhang[1,58,63], H.R. Zhang[71,58], H.Y. Zhang[1,58], J. Zhang[80], J. Zhang[59], J.J. Zhang[52], J.L. Zhang[20], J.Q. Zhang[41], J.S. Zhang[12,g], J.W. Zhang[1,58,63], J.X. Zhang[38,k,l], J.Y. Zhang[1], J.Z. Zhang[1,63], Jianyu Zhang[63], L.M. Zhang[61], Lei Zhang[42], P. Zhang[1,63], Q.Y. Zhang[34], R.Y. Zhang[38,k,l], Shuihan Zhang[1,63], Shulei Zhang[25,i], X.D. Zhang[45], X.M. Zhang[1], X.Y. Zhang[50], Y. Zhang[72], Y. T. Zhang[80], Y.H. Zhang[1,58], Y.M. Zhang[39], Yan Zhang[71,58], Yao Zhang[1], Z.D. Zhang[1], Z.H. Zhang[1], Z.L. Zhang[34], Z.Y. Zhang[76], Z.Y. Zhang[43], Z.Z. Zhang[45], G. Zhao[1], J.Y. Zhao[1,63], J.Z. Zhao[1,58], Lei Zhao[71,58], Ling Zhao[1], M.G. Zhao[43], N. Zhao[78], R.P. Zhao[63], S.J. Zhao[80], Y.B. Zhao[1,58], Y.X. Zhao[31,63], Z.G. Zhao[71,58], A. Zhemchugov[36,b], B. Zheng[72], B.M. Zheng[34], J.P. Zheng[1,58], W.J. Zheng[1,63], Y.H. Zheng[63], B. Zhong[41], X. Zhong[59], H. Zhou[50], J.Y. Zhou[34], L.P. Zhou[1,63], S. Zhou[6], X. Zhou[76], X.K. Zhou[6], X.R. Zhou[71,58], X.Y. Zhou[39], Y.Z. Zhou[12,g], J. Zhu[43], K. Zhu[1], K.J. Zhu[1,58,63], K.S. Zhu[12,g], L. Zhu[34], L.X. Zhu[63], S.H. Zhu[70], S.Q. Zhu[42], T.J. Zhu[12,g], W.D. Zhu[41], Y.C. Zhu[71,58], Z.A. Zhu[1,63], J.H. Zou[1], J. Zu[71,58]

[1] *Institute of High Energy Physics, Beijing 100049, People's Republic of China*
[2] *Beihang University, Beijing 100191, People's Republic of China*
[3] *Bochum Ruhr-University, D-44780 Bochum, Germany*
[4] *Budker Institute of Nuclear Physics SB RAS (BINP), Novosibirsk 630090, Russia*
[5] *Carnegie Mellon University, Pittsburgh, Pennsylvania 15213, U.S.A.*
[6] *Central China Normal University, Wuhan 430079, People's Republic of China*
[7] *Central South University, Changsha 410083, People's Republic of China*
[8] *China Center of Advanced Science and Technology, Beijing 100190, People's Republic of China*
[9] *China University of Geosciences, Wuhan 430074, People's Republic of China*
[10] *Chung-Ang University, Seoul, 06974, Republic of Korea*
[11] *COMSATS University Islamabad, Lahore Campus, Defence Road, Off Raiwind Road, 54000 Lahore, Pakistan*
[12] *Fudan University, Shanghai 200433, People's Republic of China*
[13] *GSI Helmholtzcentre for Heavy Ion Research GmbH, D-64291 Darmstadt, Germany*
[14] *Guangxi Normal University, Guilin 541004, People's Republic of China*
[15] *Guangxi University, Nanning 530004, People's Republic of China*
[16] *Hangzhou Normal University, Hangzhou 310036, People's Republic of China*
[17] *Hebei University, Baoding 071002, People's Republic of China*
[18] *Helmholtz Institute Mainz, Staudinger Weg 18, D-55099 Mainz, Germany*
[19] *Henan Normal University, Xinxiang 453007, People's Republic of China*
[20] *Henan University, Kaifeng 475004, People's Republic of China*
[21] *Henan University of Science and Technology, Luoyang 471003, People's Republic of China*
[22] *Henan University of Technology, Zhengzhou 450001, People's Republic of China*
[23] *Huangshan College, Huangshan 245000, People's Republic of China*
[24] *Hunan Normal University, Changsha 410081, People's Republic of China*
[25] *Hunan University, Changsha 410082, People's Republic of China*
[26] *Indian Institute of Technology Madras, Chennai 600036, India*
[27] *Indiana University, Bloomington, Indiana 47405, U.S.A.*
[28] *INFN Laboratori Nazionali di Frascati, (A)INFN Laboratori Nazionali di Frascati, I-00044, Frascati, Italy; (B)INFN Sezione di Perugia, I-06100, Perugia, Italy; (C)University of Perugia, I-06100, Perugia, Italy*
[29] *INFN Sezione di Ferrara, (A)INFN Sezione di Ferrara, I-44122, Ferrara, Italy; (B)University of Ferrara, I-44122, Ferrara, Italy*
[30] *Inner Mongolia University, Hohhot 010021, People's Republic of China*
[31] *Institute of Modern Physics, Lanzhou 730000, People's Republic of China*
[32] *Institute of Physics and Technology, Peace Avenue 54B, Ulaanbaatar 13330, Mongolia*
[33] *Instituto de Alta Investigación, Universidad de Tarapacá, Casilla 7D, Arica 1000000, Chile*
[34] *Jilin University, Changchun 130012, People's Republic of China*
[35] *Johannes Gutenberg University of Mainz, Johann-Joachim-Becher-Weg 45, D-55099 Mainz, Germany*
[36] *Joint Institute for Nuclear Research, 141980 Dubna, Moscow region, Russia*
[37] *Justus-Liebig-Universitaet Giessen, II. Physikalisches Institut, Heinrich-Buff-Ring 16, D-35392 Giessen, Germany*
[38] *Lanzhou University, Lanzhou 730000, People's Republic of China*
[39] *Liaoning Normal University, Dalian 116029, People's Republic of China*

[40] Liaoning University, Shenyang 110036, People's Republic of China
[41] Nanjing Normal University, Nanjing 210023, People's Republic of China
[42] Nanjing University, Nanjing 210093, People's Republic of China
[43] Nankai University, Tianjin 300071, People's Republic of China
[44] National Centre for Nuclear Research, Warsaw 02-093, Poland
[45] North China Electric Power University, Beijing 102206, People's Republic of China
[46] Peking University, Beijing 100871, People's Republic of China
[47] Qufu Normal University, Qufu 273165, People's Republic of China
[48] Renmin University of China, Beijing 100872, People's Republic of China
[49] Shandong Normal University, Jinan 250014, People's Republic of China
[50] Shandong University, Jinan 250100, People's Republic of China
[51] Shanghai Jiao Tong University, Shanghai 200240, People's Republic of China
[52] Shanxi Normal University, Linfen 041004, People's Republic of China
[53] Shanxi University, Taiyuan 030006, People's Republic of China
[54] Sichuan University, Chengdu 610064, People's Republic of China
[55] Soochow University, Suzhou 215006, People's Republic of China
[56] South China Normal University, Guangzhou 510006, People's Republic of China
[57] Southeast University, Nanjing 211100, People's Republic of China
[58] State Key Laboratory of Particle Detection and Electronics, Beijing 100049, Hefei 230026, People's Republic of China
[59] Sun Yat-Sen University, Guangzhou 510275, People's Republic of China
[60] Suranaree University of Technology, University Avenue 111, Nakhon Ratchasima 30000, Thailand
[61] Tsinghua University, Beijing 100084, People's Republic of China
[62] Turkish Accelerator Center Particle Factory Group, (A)Istinye University, 34010, Istanbul, Turkey; (B)Near East University, Nicosia, North Cyprus, 99138, Mersin 10, Turkey
[63] University of Chinese Academy of Sciences, Beijing 100049, People's Republic of China
[64] University of Groningen, NL-9747 AA Groningen, The Netherlands
[65] University of Hawaii, Honolulu, Hawaii 96822, U.S.A.
[66] University of Jinan, Jinan 250022, People's Republic of China
[67] University of Manchester, Oxford Road, Manchester, M13 9PL, United Kingdom
[68] University of Muenster, Wilhelm-Klemm-Strasse 9, 48149 Muenster, Germany
[69] University of Oxford, Keble Road, Oxford OX13RH, United Kingdom
[70] University of Science and Technology Liaoning, Anshan 114051, People's Republic of China
[71] University of Science and Technology of China, Hefei 230026, People's Republic of China
[72] University of South China, Hengyang 421001, People's Republic of China
[73] University of the Punjab, Lahore-54590, Pakistan
[74] University of Turin and INFN, (A)University of Turin, I-10125, Turin, Italy; (B)University of Eastern Piedmont, I-15121, Alessandria, Italy; (C)INFN, I-10125, Turin, Italy
[75] Uppsala University, Box 516, SE-75120 Uppsala, Sweden
[76] Wuhan University, Wuhan 430072, People's Republic of China
[77] Yantai University, Yantai 264005, People's Republic of China
[78] Yunnan University, Kunming 650500, People's Republic of China
[79] Zhejiang University, Hangzhou 310027, People's Republic of China
[80] Zhengzhou University, Zhengzhou 450001, People's Republic of China

[a] Deceased
[b] Also at the Moscow Institute of Physics and Technology, Moscow 141700, Russia
[c] Also at the Novosibirsk State University, Novosibirsk, 630090, Russia
[d] Also at the NRC "Kurchatov Institute", PNPI, 188300, Gatchina, Russia
[e] Also at Goethe University Frankfurt, 60323 Frankfurt am Main, Germany
[f] Also at Key Laboratory for Particle Physics, Astrophysics and Cosmology, Ministry of Education; Shanghai Key Laboratory for Particle Physics and Cosmology; Institute of Nuclear and Particle Physics, Shanghai 200240, People's Republic of China

[g] Also at Key Laboratory of Nuclear Physics and Ion-beam Application (MOE) and Institute of Modern Physics, Fudan University, Shanghai 200443, People's Republic of China
[h] Also at State Key Laboratory of Nuclear Physics and Technology, Peking University, Beijing 100871, People's Republic of China
[i] Also at School of Physics and Electronics, Hunan University, Changsha 410082, China
[j] Also at Guangdong Provincial Key Laboratory of Nuclear Science, Institute of Quantum Matter, South China Normal University, Guangzhou 510006, China
[k] Also at MOE Frontiers Science Center for Rare Isotopes, Lanzhou University, Lanzhou 730000, People's Republic of China
[l] Also at Lanzhou Center for Theoretical Physics, Key Laboratory of Theoretical Physics of Gansu Province, and Key Laboratory for Quantum Theory and Applications of MoE, Lanzhou University, Lanzhou 730000, People's Republic of China
[m] Also at the Department of Mathematical Sciences, IBA, Karachi 75270, Pakistan
[n] Also at Ecole Polytechnique Federale de Lausanne (EPFL), CH-1015 Lausanne, Switzerland
[o] Also at Helmholtz Institute Mainz, Staudinger Weg 18, D-55099 Mainz, Germany